Cancer Management and Research

Dovepress
open access to scientific and medical research

Open Access Full Text Article

ORIGINAL RESEARCH

Altered Functional Connectivity Density in Young Survivors of Acute Lymphoblastic Leukemia Using Resting-State fMRI

This article was published in the following Dove Press journal:
Cancer Management and Research

Linglong Chen[1]
Yaru Zhan[2]
Fei He[3]
Shouhua Zhang[3]
Lin Wu[2,4]
Honghan Gong[2,4]
Fuqing Zhou[2,4]
Xianjun Zeng[2,4]
Haibo Xu[1]

[1]Department of Radiology, Zhongnan Hospital of Wuhan University, Wuhan 430071, People's Republic of China; [2]Department of Radiology, The First Affiliated Hospital, Nanchang University, Nanchang 330006, People's Republic of China; [3]Department of Hematology, Jiangxi Provincial Children's Hospital, Nanchang, 330000, People's Republic of China; [4]Jiangxi Medical Imaging Research Institute, Nanchang 330006, People's Republic of China

Objective: Using functional connectivity density (FCD) mapping measured by resting-state functional magnetic resonance imaging (rs-fMRI), an ultrafast data-driven graph theory approach, we attempted to study the abnormalities in neural activity of young survivors of acute lymphoblastic leukemia (ALL) and to explore the neuropathological evidence of chemotherapy-related cognitive impairment of patients.

Methods: Twenty young survivors of ALL and 18 well-matched healthy controls (HCs) were recruited in this study. All ALL patients and healthy controls underwent rs-fMRI scans and completed neurocognitive testing. The between-group differences in short-range and long-range FCD were calculated by the option of degree centrality (DC) in MATLAB software after preprocessing. The correlations between the FCD value and each of the neurocognitive outcomes were analyzed in the ALL patients.

Results: The group-averaged FCD maps showed similar spatial patterns between the two groups. Compared with the HCs, ALL patients showed decreased long-range FCD in regions of the bilateral lingual gyrus, cingulate cortex, hippocampal gyrus, and right calcarine fissure. Simultaneously, decreased regions in the short-range FCD map were the bilateral lingual gyrus, cingulate cortex, parahippocampal gyrus and right calcarine fissure. Increased functional connectivity (FC) was observed between the region with decreased long-range FCD and the posterior cerebellar lobe, and decreased FC was observed between the region and the middle occipital gyrus, cuneus and lingual gyrus. Thus, there existed no brain areas with increased FCD. The decreased short-range FCD value of ALL patients was positively correlated with the score on the Digit Span Test (Forward), and the increased FC value was negatively correlated with the score on the Trail Making Test part A.

Conclusion: Our results suggest the altered functional connectivity of young survivors of ALL in the posterior region of the brain and posterior lobe of the cerebellum. Alterations in spontaneous neuronal activity seem to parallel the neurocognitive testing, which indicates that the rs-fMRI could be used as a neuroimaging marker for neurological impairment in ALL patients.

Keywords: acute lymphoblastic leukemia, resting-state fMRI, functional connectivity density, chemotherapy-related cognitive impairment, executive function

Correspondence: Haibo Xu
Department of Radiology, Zhongnan Hospital of Wuhan University, Wuhan, People's Republic of China
Email xuhaibo1120@hotmail.com

Honghan Gong
Department of Radiology, The First Affiliated Hospital of Nanchang University, Nanchang 330006, People's Republic of China
Email 2805794252@qq.com

Introduction

Acute lymphoblastic leukemia (ALL) is the most common malignancy in childhood. The application of chemotherapy has greatly improved the event-free survival rate and outcomes over the last few decades. However, chemotherapy drugs such as methotrexate have been shown to be neurotoxic, with disruption of astrocytes, inflammatory responses and microvascular damage.[1] Accumulating evidence has

submit your manuscript | www.dovepress.com
DovePress
http://doi.org/10.2147/CMAR.S253202

shown that chemotherapy-related cognitive impairment (CRCI) is a non-negligible issue for long-term survival states, as there are studies concerned with the deterioration of intelligence, executive function and processing speeds of adult survivors.[2,3] The childhood brain is at an important stage of growth and development for myelination, synaptogenesis and the establishment of complex neuronal connections. Resting-state magnetic resonance imaging, whether functional (fMRI) or structural, has been widely used as an objective method to understand the possible neuroimaging basis of cognitive deficits.[4–7] Survivors of ALL who have undergone chemotherapy show a reduction in fractional anisotropy,[8] smaller cortical surface area,[5] smaller white matter volumes[9,10] and altered spontaneous activity in the hippocampus,[11] accompanied by poor neurocognitive performance.

However, to date, there have been few studies aimed at measuring global functional changes in juvenile survivors of ALL. We used functional connectivity density (FCD) mapping, as a known method in relation to the spontaneous release of synaptic neurotransmitters,[12,13] aiming to determine the widespread alterations in brain function when cognitive deficits occur. Therefore, any abnormality in neural activity, such as apoptosis, and developmental, plastic, and degenerative mechanisms, would result in a change in FCD. Further, we sought to explore the relationship between the disorder of FCD and cognitive impairment in young survivors of ALL and the probable functional manifestations.

Materials and Methods

Subjects

In total, 24 young survivors of ALL and 22 age-matched healthy controls (HCs) were recruited into the study. All of the patients, who had completed standard-risk treatment based on Chinese Children Leukemia Group (CCLG)-ALL 2008, were included according to the following criteria: 1) were off-therapy for at least 12 months at the time of enrollment; 2) had received a standard chemotherapy regimen; and 3) had no history of cranial radiation, CNS involvement or gross neuropathologies. All of the HCs were recruited through community postings, and had no major sensory impairments, MRI contraindications or any significant cognitive disorders.

The results of neurocognitive scales for ALL patients and HCs, such as the intelligence quotient (IQ) (full scale of the Wechsler Adult Intelligence Scale, Fourth Edition [WAIS-IV]), Trail Making Test part A (TMT A), and Wechsler Memory Scale Digit Span Test (Forward) (DST), were collected by two experienced psychiatrists.

This study was conducted in accordance with the Declaration of Helsinki, and the Human Research Ethics Committee of the First Affiliated Hospital of Nanchang University approved the study protocol., Because all of our participants were under the age of 18 years, written informed consent was obtained from a parent or legal guardian of each participant prior to the study.

MRI Data Acquisition

The fMRI data were acquired on the same Siemens Trio 3.0 T scanner, implementing an eight-channel phased-array head coil, in the First Affiliated Hospital of Nanchang University, China. Each subject was fixed comfortably by a belt and foam pads during resting-state fMRI (rs-fMRI) scanning, keeping the supine position and with the head in a neutral position, eyes closed and awake. The rs-fMRI data were acquired with two sequences: a gradient-echo echo-plan ar imaging (EPI) sequence of 240 volumes, and high-resolution brain structural images using a T1-weighted 3D magnetization-prepared rapid gradient-echo (MP-RAGE) sequence. The parameters of the EPI sequence were: repetition time (TR)=2,000 ms, echo time (TE)=40 ms, flip angle=90°, slice thickness/gap=4.0/1 mm, field of view (FOV)=240×240 mm, in-plane resolution=64×64 and 30 axial slices to cover the whole brain; scanning time was 8 minutes. The parameters of the 3D MP-RAGE sequence were: TR=1,900 ms, TE=2.26 ms, flip angle=9°, matrix=256×256, FOV=240×240 mm, thickness=1.0 mm and 176 sagittal slices; scanning time was 3 minutes.

fMRI Data Preprocessing

Preprocessing of fMRI data was carried out using Data Processing Assistant for rsfMRI (DPARSF, http://rfmri.org/dpabi) in the MATLAB (MathWorks Inc., Natick, MA, USA) working platform. The first ten volumes of each data set were discarded for signal equilibrium. Then, slice-timing correction of temporal differences was applied to the remaining 230 volumes. The resulting images were realigned according to the first volume following a criterion of head motion within 3 mm translations and 3° rotations in any axis. Subjects were excluded if their framewise displacement (FD) exceeded 0.3, where FD was calculated as an index of head motion. Four ALL patients and four HCs were eventually excluded because of head motion parameters. Afterward, the realigned

functional data underwent co-registration based on their respective high-resolution T1-weighted structural images, then were spatially normalized to standard Montreal Neurological Institute (MNI) space with a resampled voxel size of 3×3×3 mm^3, having regressed out the nuisance variables. Finally, band-pass filtering (0.01–0.08 Hz) was performed to reduce low-frequency drifts and high-frequency physiological noise.

Resting-State FCD Calculation

Long- and short-range FCD calculations were carried out on Graph Theoretical Network Analysis (GRETNA, http://www.nitrc.org/projects/gretna/). The correlation coefficient threshold (Tc) was set to 0.25 to reduce the false-positive rate and lower the sensitivity. The rate (r) of the correlation coefficient was calculated through Pearson correlation between time-varying signals of a certain voxel and every other voxel in the gray matter (GM); these two voxels could be considered to be relative if $r>0.25$. The threshold of the signal-to-noise ratio (SNR) was set as 0.5 within the GM regions to minimize unwanted susceptibility-related signal loss. The calculation result of each voxel made up the global FCD, which means the functional connection density distribution of the whole brain (Tomasi et al, 2010).[14] According to He,[15] a connection within a given anatomical distance of 75 mm can be considered an intraregional effective functional connection, which makes up the short-range FCD. Then, the long-range FCD exists outside the region, equaling the difference between the global FCD and long-range FCD. In order for the result to be in a normal distribution, the long- and short-range FCD maps of each dataitem were rescaled by the individual average FCD value and converted to Z scores. Finally, the normalized FCD data were spatially smoothed with a Gaussian kernel of 6×6×6 mm^3 depending on full width at half maximum (FWHM), in order to increase the SNR and eliminate artifacts.

Statistical Analysis for FCD

First, the spatial distribution of mean short- and long-range FCD was estimated in the ALL group and HC group, respectively. Then, general linear model (GLM) analysis of between-group FCD comparisons was performed in DPARSF, while nuisance covariates such as age, gender and average FD were included. Two-tailed Gaussian random field (GRF) correction was used to reduce the false-positive rate, with a corrected threshold of voxel p-value <0.01, cluster p-value <0.05 and a GM mask. The mean short- and long-range FCD in clusters with significant differences between groups were further estimated by Cohen's d to determine the effect size (ES) (Mégevand et al, 2014).[16] Moreover, a partial correlation analysis, with age and gender as covariates of no interest, was performed to investigate whether the FCD in the regions showing significant group differences correlated with the outcomes of neurocognitive scales.

ROI-Based FC Calculation and Statistical Analysis

Region of interest (ROI)-based FC analysis was performed on the ROIs that showed significant differences between the ALL and HC groups in the long-range FCD. The mean time course for each ROI was extracted using DPABI (http://rfmri.org/DPARSF) and Pearson correlation coefficients of the mean time courses were calculated between pairwise ROIs for each subject. After Fisher's r-to-z transformation, calculations were performed in the following procedure. First, we used the FC values for between-group comparison only if the FC values extracted from the ROIs between ALL patients and HCs were statistically significant within each group after a random effects one-sample t-test in SPM8. Next, the z-values for all ROIs of the ALL and HC groups were evaluated by a GLM analysis in SPM8 after controlling for age and gender with the GRF correction (voxel $p<0.01$, cluster $p<0.05$). The ES was also estimated by Cohen's d to determine the significant differences between groups. Finally, we assessed the correlations between values of altered long- and short-range FCD and ROI-based rsFC in ALL patients with clinical data by partial correlation analysis.

Results

Demographic and Clinical Data

Table 1shows that the mean age of young ALL survivors was 10.15±3.1 years, and the mean duration off therapy ranged from 12 to 18 months. There were no significant differences between the two groups in age, gender or handedness.

Spatial Distribution of FCD

The group-averaged FCD maps showed similar spatial patterns in the ALL patients and HCs. There was a wide spatial extent of both long-range FCD and short-range FCD in the temporal, parietal and limbic lobes, and the

Table 1 General Clinical Information for Young Survivors of Acute Lymphoblastic Leukemia (ALL) and Healthy Controls (HCs)

Condition	ALL	HCs	*p*
Mean age (years)	10.15±3.1	9.94±3.8	>0.99
Gender (male/female)	18/2	16/2	>0.99
Handedness (right/left)	19/1	18/0	>0.99
Mean duration off therapy (months) (range)	12–18	–	n/a
Head motion(mm)	0.16±0.05	0.18±0.08	0.60
Intelligence quotient (WAIS-IV)	77.6±12.3	91±14.6	<0.05
TMT A (s)	98.6±19.16	76.1±21.04	<0.05
DST	4.2±1.15	5.9±1.01	<0.05

Abbreviations: ALL, acute lymphoblastic leukemia; HC, healthy control; –, no data; n/a, not applicable; WAIS-IV, Wechsler Adult Intelligence Scale, Fourth Edition; TMT A, TrailMaking Test A; DST, Digit Span Test.

cuneus. Besides, short-range FCD was higher in the precuneus and cingulate, and long-range FCD was observed to be higher in the postcentral, precentral and medial frontal gyrus (Figure 1).

Group Differences in FCD

A between-group comparison was conducted to reveal differences in long-range FCD and short-range FCD (Table 2; Figure 2). Compared with the HCs, decreased regions in the long-range FCD map were the bilateral lingual gyrus, cingulate cortex, parahippocampal gyrus and right calcarine fissure. Simultaneously, decreased regions in the short-range FCD map were the bilateral cuneus, lingual gyrus, cingulate cortex, hippocampal gyrus and precuneus (GRF correlation, cluster $p<0.01$, voxel $p<0.05$).

Alteration in FC Based on Seed Region

The region of the bilateral lingual gyrus, cingulate cortex, parahippocampal gyrus and right calcarine fissure, which showed a decreased long-range FCD, was defined as an

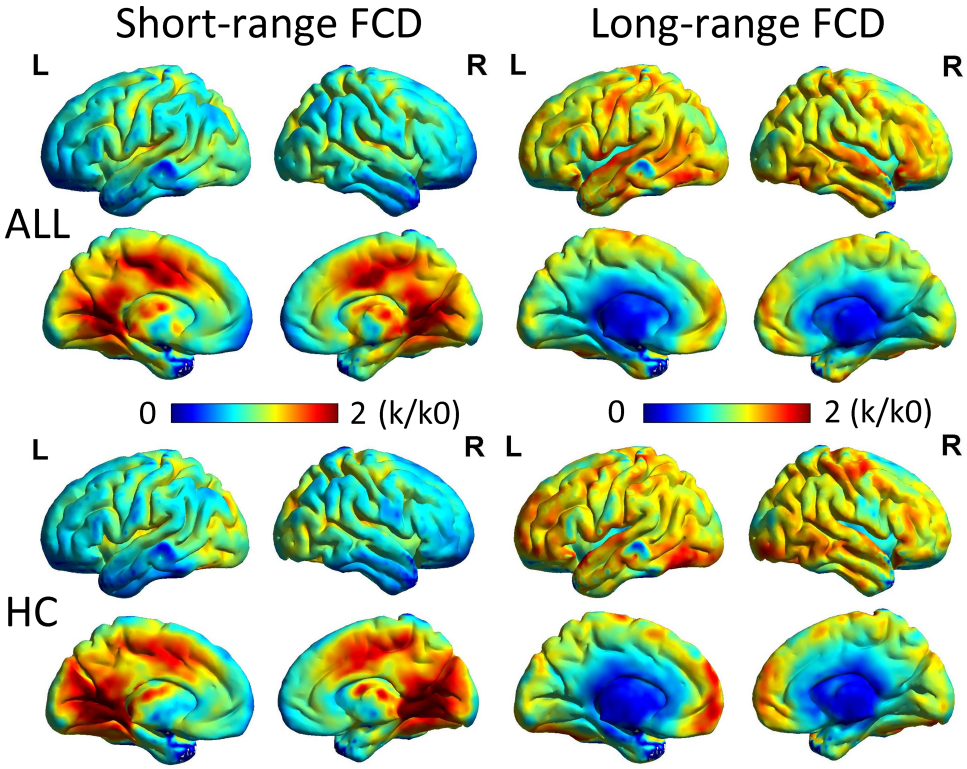

Figure 1 Spatial distribution of short- and long-range FCD in ALL and HCs, visualized with the BrainNet Viewer (http://www.nitrc.org/projects/bnv/).
Abbreviations: FCD, functional connectivity density; L, left; R, right; ALL, acute lymphoblastic leukemia; HC, healthy control; k/k0, normalized FCD.

Table 2 Differences in Short-Range FCD and Long-Range FCD Between the ALL and HC Groups (GRF Correction, Voxel-Wise $p<0.01$, Cluster-Wise $p<0.05$)

Brain Region (BA)	Cluster Size (Voxels)	MNI Coordinates			Peak T value	ES
		x	y	z		
Decreased short-range FCD						
Bilateral LING/CC/HIP/R CAL (BA 47/31/33/39/44)	789	42	−87	−6	−5.3	1.85
Decreased long-range FCD						
Bilateral CUN/LING/CC/PHG/preCUN (BA 46/47/31/33/39/67)	425	15	−39	−9	−4.7	1.08

Note: A negative T value means that the resting-state FCD in ALL is smaller than in HCs.
Abbreviations: FCD, functional connectivity density; ALL, acute lymphoblastic leukemia; HC, healthy control; GRF, Gaussian random field; BA, Brodmann area; LING, lingual gyrus; CC, cingulate cortex; HIP, hippocampus; R, right; CAL, calcarine fissure and surrounding cortex; CUN, cuneus; PHG, parahippocampal gyrus; preCUN, precuneus; MNI, Montreal Neurological Institute; ES, effect size.

ROI. Table 3 and Figure 3 show the between-group results of FC: there was significantly increased FC between ROI and the posterior cerebellar lobe, and decreased FC between ROI and the middle occipital gyrus, cuneus and lingual gyrus in ALL patients.

Correlations

The decreased short-range FCD value of ALL patients was positively correlated with the score on the DST ($r=0.5$, $p<0.05$) and the increased rsFC value was negatively correlated with the score on the TMT A ($r=0.7$, $p<0.05$), as shown in Figure 4.

Discussion

As far as we know, this is the first study to apply FCD mapping to investigate the altered spontaneous neuronal activity of young survivors of ALL. Our results indicate that there is some overlap between long- and short-range FCD in the lingual gyrus and cingulate cortex, which reflects the considerable degree of functional disruption in these regions. Besides, altered FCD occurred in the cingulate cortex, parahippocampal and hippocampal gyrus, right calcarine fissure, cuneus and precuneus, indicating that chemosensitivity or toxicity may be more pronounced in the posterior region of the brain. Previous studies were more concerned with structural changes in ALL showing widespread alterations.[5,6] Genschaft et al found smaller volumes in the left calcarine gyrus, both lingual gyri and the left precuneus, smaller hippocampal volumes and lower figural memory.[17] Therefore, structural abnormalities probably give rise to local and remote FCD changes.

Previous studies suggested that receiving chemotherapy at a younger age may be predictive of poor neurocognitive outcomes.[18,19] A decline in the cognitive performance of cancer survivors was confirmed in intelligence, attention, working memory, executive function and other aspects.[18] For patients in our study, the poor performance on the DST was negatively correlated with the short-range FCD value of the bilateral lingual gyrus, cingulate cortex, hippocampal gyrus and right calcarine fissure. The DST is a measure of working memory, especially short-term memory and attention. Impaired neurocognitive function of ALL patients can be measured using this neurocognitive scale.

The pathophysiology of methotrexate-induced neurotoxicity is associated with oxidative stress injury of vascular endothelial cells and neurons, diffuse demyelination and myelin formation disorders of white matter.[2,3] CRCI caused by other commonly used drugs is considered to be related to glial progenitor cell death, destruction of the microvasculature and so on.[20–22] A previous study clarified the hippocampal toxicity of chemotherapy and hippocampal-dependent brain plasticity.[23] Considering the important role of the hippocampus in memory formation, memory maintenance, learning and anxiety, Monje and Dietrich reported reduced hippocampal atrophy and increased BOLD signal in the hippocampus during an unsuccessful encoding task.[11] In the resting state, Kesler et al found altered clustered connectivity in hippocampal and occipital regions, and lower IQ was related to decreased FC between the left hippocampus and left lingual gyrus.[24] In addition to decreased hippocampal volumes with lower figural memory in Genschaft's study, another group of survivors of ALL showed decreased hippocampal GM with reduced verbal learning/memory.[25] Combined with our result of suppressed spontaneous hippocampal activity, in proportion

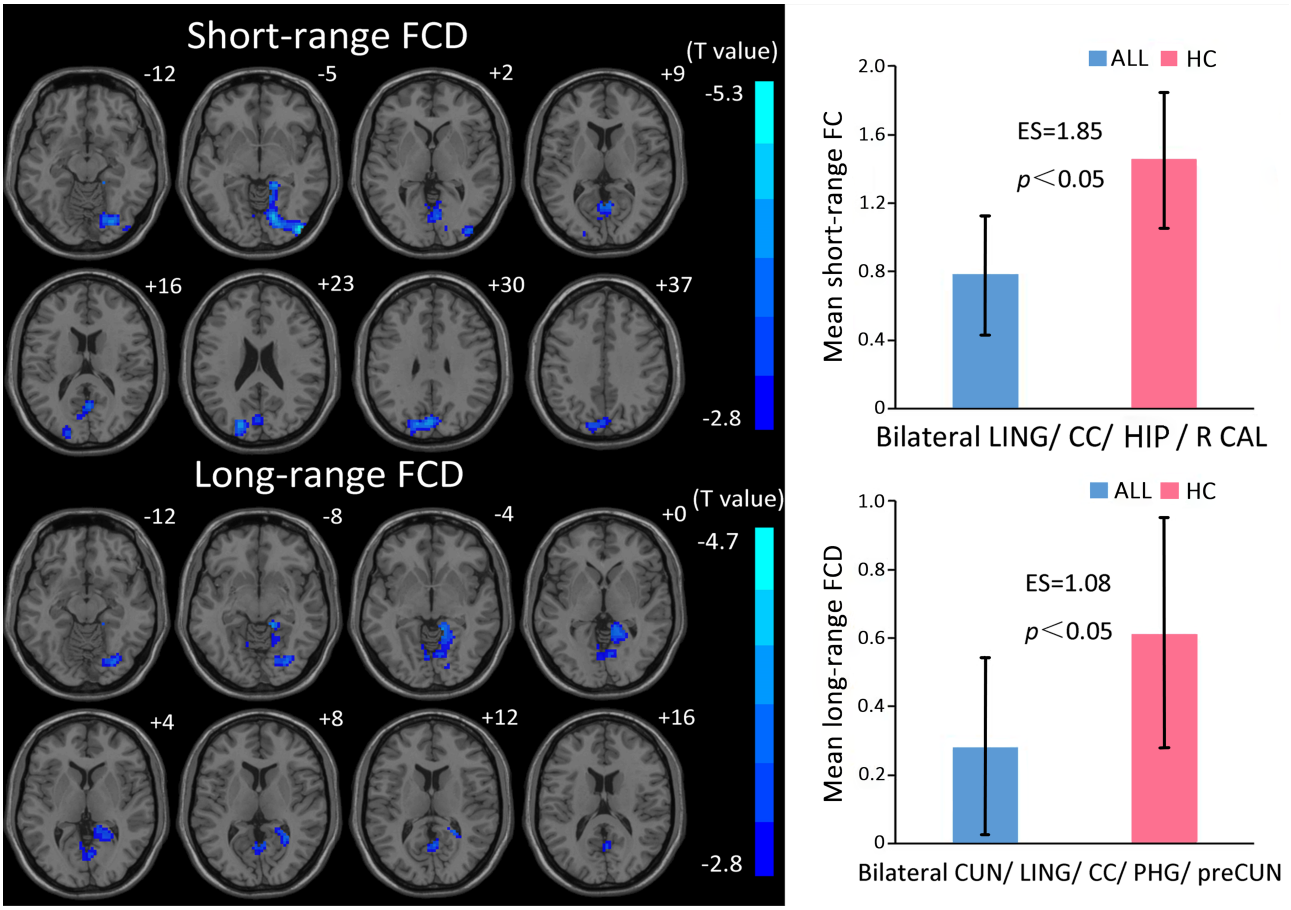

Figure 2 Brain regions with significant changes in short- or long-range FCD in ALL (voxel $p<0.01$, cluster $p<0.05$, GRF corrected), visualized with the DPABI slice viewer (http://rfmri.org/dpabi).

Notes: A negative T value means that the resting-state FCD in ALL is smaller than in HCs. Significant group differences in the mean strength of the short- (above) and long-range (below) FCD in the above regions ($p<0.05$). The error bars are standard errors of the mean.

Abbreviations: FCD, functional connectivity density; ALL, acute lymphoblastic leukemia; HC, healthy control; GRF, Gaussian random field; LING, lingual gyrus; CC, cingulate cortex; HIP, hippocampal gyrus; R, right; CAL, calcarine fissure and surrounding cortex; CUN, cuneus; PHG, parahippocampal gyrus; preCUN, precuneus; ES, effect size.

to working memory, we can hypothesize that maladaptive hippocampal functioning and disordered functional networks may be the pathophysiological cause of memory impairment.

In a previous study, Tomasi and Volkow indicated that the precuneus was the region with the highest short-range FCDs and significant long-range FCDs in healthy people.[26] The

Table 3 Differences in Functional Connectivity Between the ALL and HC Groups (GRF Correction, Voxel-Wise $p<0.01$, Cluster-Wise $p<0.05$)

Brain Region (BA)	Cluster Size (Voxels)	MNI Coordinates			Peak T value	ES
		x	y	z		
Seed: CUN/LING/CC/PHG/preCUN						
Increased FC: CbPL (lobule crus I/VIIIa/VIIIb/IX)	392	6	−48	−51	3.6598	0.3031
Decreased FC: MOG/CUN/LING (BA 7/46/47)	329	−15	−81	−3	−3.3558	1.008

Notes: A positive T value means that the resting-state FC in ALL is larger than in HCs; a negative T value means that the resting-state FC in ALL is smaller than in HCs.

Abbreviations: ALL, acute lymphoblastic leukemia; HC, healthy control; GRF, Gaussian random field; BA, Brodmann area; CUN, cuneus; LING, lingual gyrus; CC, cingulate cortex; PHG, parahippocampal gyrus; preCUN, precuneus; FC, functional connectivity; CbPL, cerebellum posterior lobe; MOG, middle occipital gyrus; MNI, Montreal Neurological Institute; ES, effect size.

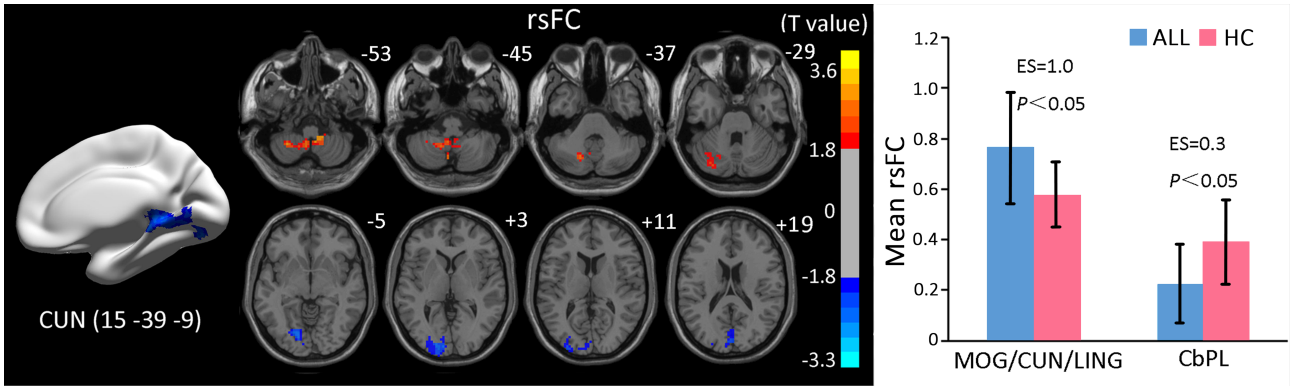

Figure 3 Brain regions with significant changes in rsFC with the bilateral CUN/LING/CC/PHG/preCUN in ALL (voxel $p<0.01$, cluster $p<0.05$, corrected), visualized with the DPABI slice viewer (http://rfmri.org/dpabi).
Note: Significant group differences in the mean strength of rsFC in the above regions ($p<0.05$). The error bars are standard errors of the mean.
Abbreviations: rsFC, resting-state functional connectivity; ALL, acute lymphoblastic leukemia; HC, healthy control; MOG, middle occipital gyrus; CUN, cuneus; LING, lingual gyrus; CbPL, posterior cerebellar lobe.

precuneus, the key node (hub) in the default brain functional network, which is associated with conscious recall of short-term memory, is vulnerable to oxidative stress injury. Young survivors of ALL in our study showed decreased long-range FCD in the precuneus. Research using voxel-based morphometry revealed decreased GM volume in the precuneus.[28] On the other hand, functional and structural research in brain cancer patients could be included for reference, since CRCI has also been reported in breast cancer patients after chemotherapy hwhen neurotoxic drugs such as methotrexate and fluorouracil were included in the regimen. For instance, Conroy et al revealed lower working memory-related activation in the right precuneus in breast cancer patients.[28] Wang et al demonstrated that there was compensatory increased FC between the precuneus and dorsolateral prefrontal cortex.[29] Contradictory findings may be related to altered connectivity and confusion of physiological functions in the precuneus after chemotherapy.

With the ROI of altered long-range FCD regions, we also documented significantly increased FC in the posterior lobe of the cerebellum (lobule crus I/VIIIa/VIIIb/IX). Lobule VIIIa of the cerebellum is a region associated with visuospatial attention and working memory, and patients with lesions to VIIIa (and to crus I and crus II) showed attention disorder.[30] Similar enhanced activation was also reported in breast cancer survivors, who showed increased cerebral blood flow of the

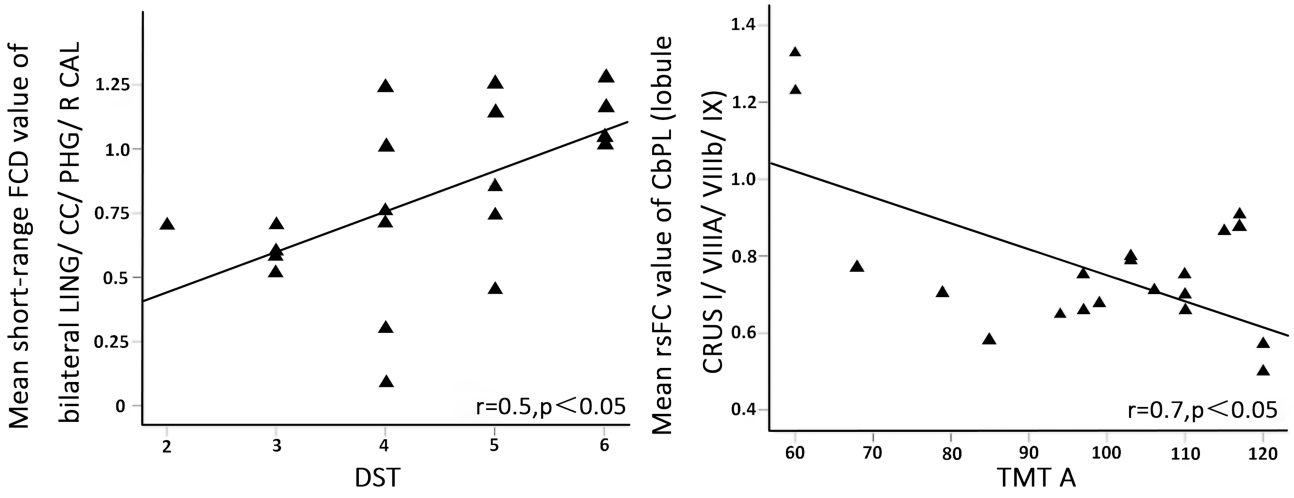

Figure 4 Relationships between clinical indices and FCD and rsFC value in ALL.
Note: The score on the DST was positively correlated with the increased rsFC value, and the score on TMT A was negatively correlated with the decreased FCD value of ALL patients.
Abbreviations: FCD, functional connectivity density; rsFC, resting-state functional connectivity; ALL, acute lymphoblastic leukemia; DST, Digit Span Test; TMT A, Trail Making Test A; LING, lingual gyrus; CC, cingulate cortex; PHG, parahippocampal gyrus; R, right; CAL, calcarine fissure and surrounding cortex; CbPL, posterior cerebellar lobe.

posterior cerebellum during a short-term word-pair association task using positron emission tomography (PET)[31] and increased BOLD signal in the resting state using fMRI.[32] In early imaging work by Kingma et al, children with ALL after chemotherapy showed a volume reduction in the cerebellum.[33] Our results indicated a correlation between increased FC in the posterior lobe of the cerebellum and patients' performance on the TMT A, so we supposed that the increased activation in the cerebellum was a kind of compensation in ALL patients.

Thus, we used the method of FCD mapping to characterize the effects of chemotherapy on brain functional networks in young survivors of ALL. The objective description of neuroimaging and brain activity could help us to understand better the unique pattern of cognitive impairment associated with chemotherapy and the potential mechanisms for compensation. However, there are two limitations to our study. First, the sample size is relatively small, which may increase false-positive and false-negative findings. Secondly, the cognitive function scale adopted did not cover all aspects of neurocognitive function.

Conclusion

Our results suggest the altered functional connectivity of young survivors of ALL in the posterior region of the cerebrum and posterior lobe of the cerebellum. Alterations in spontaneous neuronal activity seem to parallel the neurocognitive testing, which indicates that rs-fMRI could be used as a neuroimaging marker for neurological impairment in ALL patients.

Funding

This study was funded by the National Natural Science Foundation of China, Grant/Award Number: 8166070125.

Disclosure

The authors report no conflicts of interest in this work.

References

1. Monje M, Thomason ME, Rigolo L, et al. Functional and structural differences in the hippocampus associated with memory deficits in adult survivors of acute lymphoblastic leukemia. *Pediatr Blood Cancer*. 2013;60:293–300. doi:10.1016/j.bbr.2011.05.012
2. Krull KR, Brinkman TM, Li C, et al. Neurocognitive outcomes decades after treatment for childhood acute lymphoblastic leukemia: a report from the St Jude Lifetime Cohort Study. *J Clin Oncol*. 2013;31:4407–4415. doi:10.1200/JCO.2012.48.2315
3. Brinkman TM, Krasin MJ, Liu W, et al. Long-term neurocognitive functioning and social attainment in adult survivors of pediatric CNS tumors: results from the St Jude Lifetime Cohort Study. *J Clin Oncol*. 2016;34:1358–1367. doi:10.1200/JCO.2015.62.2589
4. Edelmann MN, Krull KR, Liu W, et al. Diffusion tensor imaging and neurocognition in survivors of childhood acute lymphoblastic leukaemia. *Brain*. 2014;137:2973–2983. doi:10.1093/brain/awu230
5. Tamnes CK, Zeller B, Amlien IK, et al. Cortical surface area and thickness in adult survivors of pediatric acute lymphoblastic leukemia. *Pediatr Blood Cancer*. 2015;62:1027–1034. doi:10.1002/pbc.25386
6. Kesler SR, Gugel M, Huston-Warren E, Watson C. Atypical structural connectome organization and cognitive impairment in young survivors of acute lymphoblastic leukemia. *Brain Connect*. 2016;6(4):273–282. doi:10.1089/brain.2015.0409
7. van der Plas E, Schachar RJ, Hitzler J, et al. Brain structure, working memory and response inhibition in childhood leukemia survivors. *Brain Behav*. 2017;7:e00621. doi:10.1002/brb3.621
8. Morioka S, Morimoto M, Yamada K, et al. Effects of chemotherapy on the brain in childhood: diffusion tensor imaging of subtle white matter damage. *Neuroradiology*. 2013;55:1251–1257. doi:10.1007/s00234-013-1245-7
9. Reddick WE, Shan ZY, Glass JO, et al. Smaller white-matter volumes are associated with larger deficits in attention and learning among long-term survivors of acute lymphoblastic leukemia. *Cancer-Am Cancer Soc*. 2006;106:941–949. doi:10.1002/cncr.21679
10. Reddick WE, Taghipour DJ, Glass JO, et al. Prognostic factors that increase the risk for reduced white matter volumes and deficits in attention and learning for survivors of childhood cancers. *Pediatr Blood Cancer*. 2014;61:1074–1079. doi:10.1002/pbc.24947
11. Monje M, Dietrich J. Cognitive side effects of cancer therapy demonstrate a functional role for adult neurogenesis. *Behav Brain Res*. 2012;227:376–379. doi:10.1002/pbc.24263
12. Fox MD, Raichle ME. Spontaneous fluctuations in brain activity observed with functional magnetic resonance imaging. *Neuroscience*. 2007;8:700–711. doi:10.1038/nrn2201
13. Zhang J, Bi W, Zhang Y, et al. Abnormal functional connectivity density in Parkinson's disease. *Behav Brain Res*. 2015;280:113–118. doi:10.1016/j.bbr.2014.12.007
14. Tomasi D, Volkow ND. Functional connectivity density mapping. *Proceedings of the National Academy of Sciences*. 2010;107:9885–9890. doi:10.1073/pnas.1001414107
15. He Y, Chen ZJ, Evans AC. Small-world anatomical networks in the human brain revealed by cortical thickness from MRI. *Cereb Cortex*. 2007;17:2407–2419. doi:10.1093/cercor/bhl149
16. Mégevand P, Groppe DM, Goldfinger MS, et al. Seeing Scenes: Topographic Visual Hallucinations Evoked by Direct Electrical Stimulation of the Parahippocampal Place Area. *J Neurosci*. 2014;34:5399–5405. doi:10.1523/JNEUROSCI.5202-13.2014
17. Genschaft M, Huebner T, Plessow F, et al. Impact of chemotherapy for childhood leukemia on brain morphology and function. *PLoS One*. 2013a;8:e78599. doi:10.1371/journal.pone.0078599
18. Khong PL, Kwong DL, Chan GC, Sham JS, Chan FL, Ooi GC. Diffusion-tensor imaging for the detection and quantification of treatment-induced white matter injury in children with medulloblastoma: a pilot study. *AJNR Am J Neuroradiol*. 2003;24:734–740.
19. Jacola LM, Krull KR, Pui C, et al. Longitudinal Assessment of Neurocognitive Outcomes in Survivors of Childhood Acute Lymphoblastic Leukemia Treated on a Contemporary Chemotherapy Protocol. *J CLIN ONCOL*. 2016;34:1239–1247. doi:10.1200/JCO.2015.64.3205
20. Krull KR, Bhojwani D, Conklin HM, et al. Genetic mediators of neurocognitive outcomes in survivors of childhood acute lymphoblastic leukemia. *J Clin Oncol*. 2013;31:2182–2188. doi:10.1200/JCO.2012.46.7944
21. Kaiser J, Bledowski C, Dietrich J. Neural correlates of chemotherapy-related cognitive impairment. *Cortex*. 2014;54:33–50. doi:10.1016/j.cortex.2014.01.010

22. Kesler SR, Ogg R, Reddick WE, et al. Brain network connectivity and executive function in long-term survivors of childhood acute lymphoblastic leukemia. *Brain Connect*. 2018;8:333–342. doi:10.1089/brain.2017.0574
23. Dietrich J, Prust M, Kaiser J. Chemotherapy, cognitive impairment and hippocampal toxicity. *Neuroscience*. 2015;309:224–232. doi:10.1016/j.neuroscience.2015.06.016
24. Kesler SR, Gugel M, Pritchard-Berman M, et al. Altered resting state functional connectivity in young survivors of acute lymphoblastic leukemia. *Pediatr Blood Cancer*. 2014;61:1295–1299. doi:10.1002/pbc.25022
25. Zeller B, Tamnes CK, Kanellopoulos A, et al. Reduced neuroanatomic volumes in long-term survivors of childhood acute lymphoblastic leukemia. *J Clin Oncol*. 2013;31:2078–2085. doi:10.1200/JCO.2012.47.4031
26. Tomasi D, Volkow ND. Aging and functional brain networks. *Mol Psychiatr*. 2012;17:549–558. doi:10.1038/mp.2011.81
27. Zou L, Su L, Xu J, et al. Structural brain alteration in survivors of acute lymphoblastic leukemia with chemotherapy treatment: a voxel-based morphometry and diffusion tensor imaging study. *Brain Res*. 2017;1658:68–72. doi:10.1016/j.brainres.2017.01.017
28. Conroy SK, McDonald BC, Smith DJ, et al. Alterations in brain structure and function in breast cancer survivors: effect of post-chemotherapy interval and relation to oxidative DNA damage. *Breast Cancer Res Treat*. 2013;137:493–502. doi:10.1007/s10549-012-2385-x
29. Wang L, Yan Y, Wang X, et al. Executive function alternations of breast cancer patients after chemotherapy: evidence from resting-state functional MRI. *Acad Radiol*. 2016;23:1264–1270. doi:10.1016/j.acra.2016.05.014
30. Brissenden JA, Tobyne SM, Osher DE, Levin EJ, Halko MA, Somers DC. Topographic cortico-cerebellar networks revealed by visual attention and working memory. *Curr Biol*. 2018;28:3364–3372.e5. doi:10.1016/j.cub.2018.08.059
31. Silverman DHS, Dy CJ, Castellon SA, et al. Altered frontocortical, cerebellar, and basal ganglia activity in adjuvant-treated breast cancer survivors 5–10 years after chemotherapy. *Breast Cancer Res Tr*. 2007;103:303–311. doi:10.1007/s10549-006-9380-z
32. Kesler SR, Bennett FC, Mahaffey ML, Spiegel D. Regional brain activation during verbal declarative memory in metastatic breast cancer. *Clin Cancer Res*. 2009;15:6665–6673. doi:10.1158/1078-0432.CCR-09-1227
33. Kingma A, van Dommelen RI, Mooyaart EL, Wilmink JT, Deelman BG, Kamps WA. Slight cognitive impairment and magnetic resonance imaging abnormalities but normal school levels in children treated for acute lymphoblastic leukemia with chemotherapy only. *J Pediatr*. 2001;139:413–420. doi:10.1067/mpd.2001.117066